International Journal of Concrete Structures and Materials

RESEARCH Open Access

The Effect of the Aggregate Size and Ambient Temperature on the Impact Resistance of Concrete

Cevdet Emin Ekinci[1*] and Belkis Elyigit[1]

Abstract

In this study, the effect of aggregate size and ambient temperature on the impact resistance of concrete was investigated experimentally. Also, it was tried to determine the behavior of normal and crushed stones in impact resistance, freeze–thaw, and compressive strength when used separately and together in concrete. No additives were used in the concrete samples. The consistency stability of fresh concrete is 80 mm. The D_{max} of the aggregates is 16 mm and 31.5 mm. These specimens underwent successive impact tests at temperatures of 30 °C, 0 °C, and − 25 °C and were subjected to drops from heights of 25 cm and 30 cm. The resistance of the concretes to pressure and impact increased with a larger aggregate size. Notably, concrete samples containing crushed stone exhibited higher resistance to impact compared to those with normal aggregates. On moderate, the concrete samples at temperatures of 30 °C, 0 °C, and − 25 °C could withstand 12–14, 10–12, and 6–11 consecutive impacts, respectively. A discernible decrease in the resistance of concrete against pressure and impact was observed as the atmospheric temperature decreased.

Keywords Impact resistance, Freezing–thawing, Compressive strength, Concrete, Crushed-stone

1 Introduction

The fundamental elements of concrete include aggregate, water, and cement. When combined in appropriate and optimal ratios, these elements form an artificial stone with a composite structure, commonly referred to as concrete. Concrete is a man-made stone that is formed by combining aggregate, water, and cement in inappropriate and ideal ratios. However, it is vulnerable to various detrimental influences during its application, such as temperature changes, cycles of freezing and thawing, wetting and drying conditions, and external events like earthquakes, frictional wear, static and dynamic loads, bending-tensile forces, and impacts. These factors can cause degradation of concrete's physical, chemical, and mechanical properties (Cantwell & Morton, 1991; Ekinci, 2020, 2021; Fabbro et al., 2021). In recent years, it has been adopted that impact resistance is as paramount a criterion as compressive strength in concrete and reinforced concrete structures (Oltulu & Altun, 2018; Wan et al., 2016). Apart from these external effects, concrete is also impacted by incidents like earthquakes, frictional wear, static and dynamic loads, bending-tensile forces, and impacts, causing it to lose its physical and mechanical attributes. Hence, three critical properties are sought in concrete: workability, strength, and durability. While workability is pertinent to fresh concrete, strength, and durability are relevant to hardened concrete, particularly in the context of reinforced concrete structures. Ductility, rigidity, and durability are especially vital technical characteristics in reinforced concrete buildings, and their stability is directly linked to the material properties and proportions employed in concrete production. The

Journal information: ISSN 1976-0485 / eISSN 2234-1315

*Correspondence:
Cevdet Emin Ekinci
cee@firat.edu.tr
[1] Department of Civil Engineering, Firat University, Elazig 23000, Türkiye

quality of concrete is commonly evaluated based on its resistance, defined as the maximum capacity of concrete to withstand structural changes and fractures resulting from applied loads (Wong, 2022). In common cases involving impacts, such as objects falling from a height or sudden forces, concrete structures like roads, harbors, railway facilities, and airfields are often exposed to these forces. Additionally, multi-story reinforced concrete buildings and infrastructure elements like piles and sheet pile heads may face successive impacts, particularly during seismic events. Significant stresses are induced in objects subjected to impact, and these stresses attain high magnitudes in a short duration. The rapid application of force tests the cohesive strength of the material, which plays a crucial role in withstanding object impacts. If stresses and deformations extend beyond the elastic region due to impact, they assume a complex form that may defy solutions through conventional equations. Over time, the concrete's diminishing capacity to undergo deformation results in reduced impact resistance as the material ages (Ekinci, 2006; Ekinci & Kelesoglu, 2014; Yildirim & Ekinci, 2006, 2012; Yildirim et al., 2010, 2015).

The term "impact resistance" indicates the ability of concrete to endure repeated impacts, absorbing energy without adverse effects such as cracking and spalling (Drathi, 2015). The material's resistance to impact depends on three primary factors: the velocity of force application, the severity of stress concentration within

Table 1 Physical and chemical properties of the cement

Chemical properties		**Physical properties**	
Chemical composition (%)	**CEM II/A-P**	**Specific gravity (g/cm^3)**	**3.10**
SiO_2	20.50	Specific surface (m^2/kg)	3490
Al_2O_3	5.68	Main components (~) and modules	
Fe_2O_3	3.35	C_3S	63
CaO	62.92	C_2S	12
MgO	2.80	C_3A	9
SO_3	2.05	C_4AF	10
Ignition loss	1.60	Silica module (SM)	2.27
Unidentified	0.80	Hydraulic module (HM)	2.13
Insoluble residue	0.30	Alumina module (AM)	1.69
Total	100	Lime standard (LS)	95

Table 2 Physical properties of the aggregate

Aggregate classes	**Unit weight (compressed) (kg/m^3)**	**Specific gravity (SSD) ((g/cm^3)**	**Water absorption (%)**	**Current humidity (%)**	**Abrasion (%) (all-in)**	
					100 Cycle	**500 Cycle**
0–4.0 mm	1760	2.68	1.12	0.70	6.95	18.50
4–16 mm	1730	2.71	0.85	0.50		
16–31.5 mm	1700	2.82	0.79	0.45		

Table 3 Aggregate granulometry used in experiments (percentage)

D_{max} (mm)	**0.25**	**0.50**	**1**	**2**	**4**	**8**	**16**	**31.5**
N16	10	20	30	40	60	80	100	
N31.5	10	20	25	35	50	60	80	100
C16	10	20	30	40	60	40 + 40	50 + 50	
C31.5	10	20	25	35	50	30 + 30	40 + 40	50 + 50
CN16	10	20	30	40	60	40 + 40	50 + 50	
CN31.5	10	20	25	35	50	30 + 30	40 + 40	50 + 50

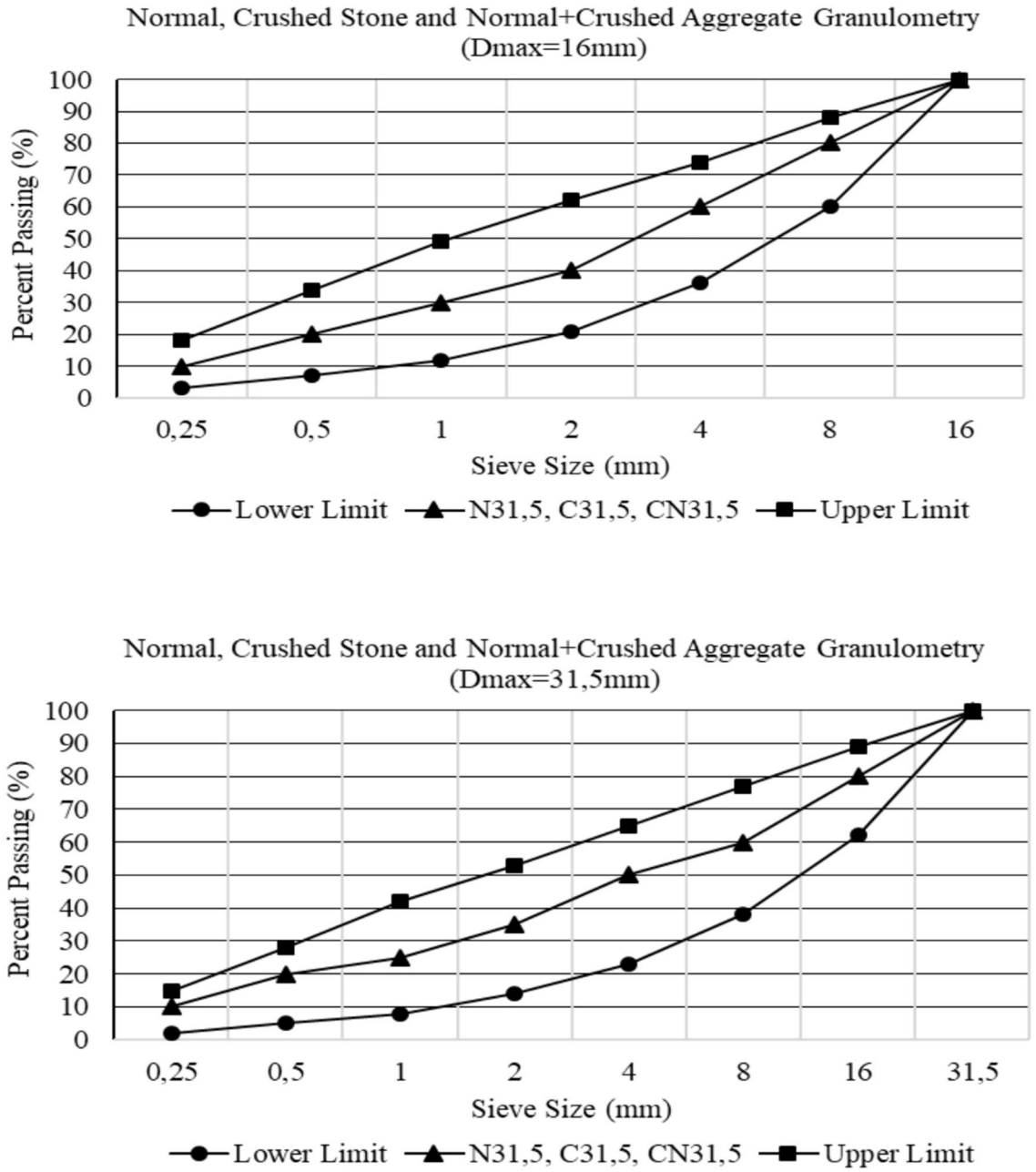

Fig. 1 Aggregate granulometry used in experiments (percentage, D_{max} = 16 mm and D_{max} = 31.5 mm)

the object, and the material's temperature. Another strategy to enhance impact resistance is by increasing the material's toughness and ductility. The impact resistance of concrete holds significant importance in diverse applications, including industrial floors, hydraulic structures, and explosion-proof constructions (Moein et al., 2022; Oltulu & Altun, 2018; Wan et al., 2016). Additionally, the concrete's impact resistance is intricately linked to the area beneath its stress–unit deformation curve, representing its toughness. The extent of this area is influenced not only by the material's high resistance, but also by its ductility. Given that concrete is generally considered a brittle material, its resistance is subject to change based on factors like the mortar matrix and the quality of the intermediate surface (Dok et al., October 2020; Yang et al., 2012). In regions with cold climates, concrete structures undergo degradation of quality and properties due to

Table 4 Concrete mixture proportions

D_{max} (mm)	W/C	PC (kg)	Mixing water (lt))	Aggregate (kg)			
				0–4	4–16	4–31.5	Total
N16	0.55	326	179	758	1197	–	2460
N31.5	0.51	346	176	754	–	1191	2467
C16	0.55	326	179	758	1197	–	2460
C31.5	0.51	346	176	754	–	1191	2467
CN16	0.55	326	179	758	1197	–	2460
CN31.5	0.51	346	176	754	–	1191	2467

freeze–thaw cycles over their lifespan. However, the incorporation of an air-entraining agent in concrete can enhance its resistance to freezing and thawing (Etman & Ahmed, 2018). Several experimental studies on the freeze–thaw behavior of concrete have highlighted key findings. These results can be summarized as follows: enhancing concrete frost resistance primarily involves reducing the macro capillary consistency of hardened cement paste and forming stable gel-like hydration products. Cyclic freezing contributes to concrete deterioration through temperature-induced stresses and deformations (Wang et al., 2021; Ya Trofimov et al., 2017). Higher relative humidity promotes the hydration of cementitious materials (Suryawanshi et al., 2022). Concrete subjected to a freeze–thaw cycle at an early age may experience significant physical damage, leading to a decline in its performance (Liu et al., 2021; Wang et al., 2022). The amount of coarse aggregate in concrete affects its strength, elastic modulus, thermal properties, and resistance to chloride dispersion (Saleem et al., 2021; Yang & Dai, 2020). The objective of the present study is to lead experimental examinations of the mechanical behaviors of concrete subjected to consecutive impact effects under different ambient temperatures and with varying aggregate sizes.

Exposure of concrete to high temperatures causes changes in its physical and chemical properties as well as a decrease in its mechanical properties such as compressive strength and modulus of elasticity. As a result, the structural resistance capacity and the stability of the system are compromised (Georgali & Tsakiridis, 2005; Guo & Shi, 2011; Hager, 2013a; Hourt, 2000). Deterioration of these properties directly depends on material-related factors (aggregate and cement type, water/cement ratio, additives, and fibers) and the environment (fire exposure time, heat generation rate, applied load, and humidity) (Fédération internationale du béton – FIB., 2007; Hager, 2013a; Hourt, 2000). Analysis of this degradation helps to diagnose the structure and define repair, strengthening, and even demolition

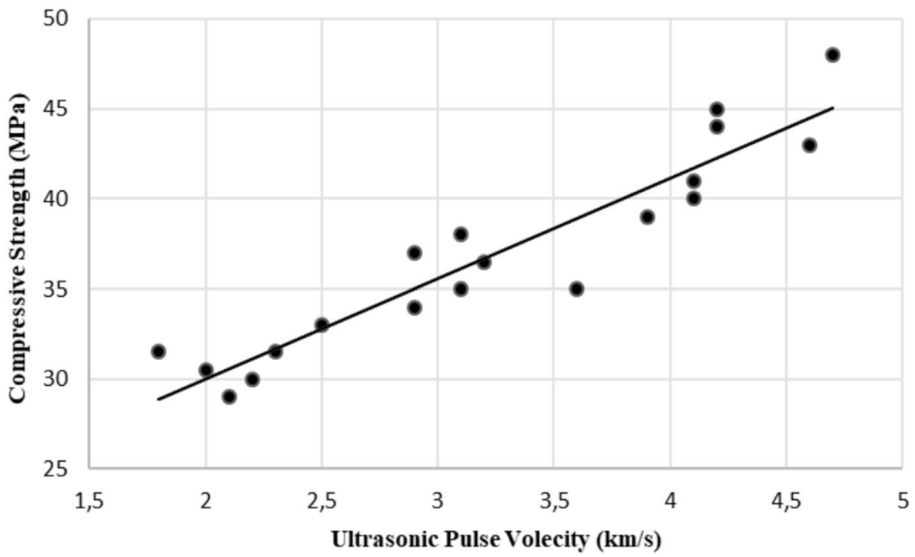

Fig. 2 Converting concrete impact strength test results to equivalent cube compressive strength

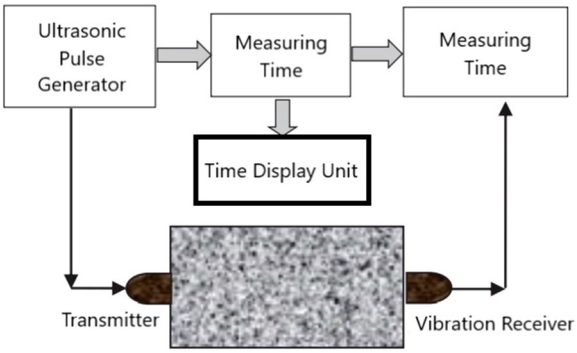

Fig. 3 Ultrasound method (UPTV) in concrete compressive strength determination (Zebari et al., 2017)

strategies (Fédération internationale du béton – FIB., 2008; Hager, 2013b).

Concretes face different behaviors where they are used. These are issues such as wear (Li et al., 2021; Niță et al., 2023; Warudkar & Elavenil, 2020), freeze–thaw (Luo et al., 2022; Wang et al., 2022, 2023), impact (Alwesabi et al., 2020; Pham et al., 2020; Zhang et al., 2021), harmful chemicals (Rafieizonooz et al., 2020; Raghav et al., 2021; Wang et al., 2020). These issues negatively affect the physical and mechanical properties of concrete.

2 Materials

2.1 Cement

The CEM II/A-P cement used in this study was supplied by Elazig Cement Factory. Physical and chemical analysis results of the mentioned cement are given in Table 1 according to TS EN 197–1 (En&197–1, 2012) standards.

2.2 Aggregate

In experimental studies, the Elazığ-Palu District of aggregate (Turkiye) was used. All the aggregates used in the experiments were tested with compliance with the TS706 EN12620+A1 (TS 706 EN, 12620+A1 2009) and TS 699 (TS699, 2009) requirements and no softening and dispersing were observed under the effect of water. The physical properties of the aggregates and their results in granulometric percentage (%) are shown in Tables 2–3 and Fig. 1.

2.3 Mixing Water

Elazig City water which has a 7.5pH value, was utilized as the concrete mixing water. The water was allowed to rest in the laboratory for one full day to reach a stable temperature of 20 ± 3 °C before being used for mixing.

2.4 Concrete Classes

Six different concrete classes were used in experimental studies. These are N16, N31.5, C16, C31.5, CN16 and CN31.5. Concrete mixing ratios are given in Table 4.

3 Experimental Method

Initially, various parameters such as aggregate granulation, granulometry curves (sieve curves), fineness module, and specific surface, along with water demand coefficients, were determined. Afterward, the upper and lower grain quantities for all grain classes, excluding mixed aggregate, were identified in volumetric percentages based on three sieve openings (0–16 and 0–31.5) according to the standards outlined in TS 706 EN 12620+A1. The produced concretes for the experiments were categorized according to the D_{max} status (e.g., N16, C16, and CN31.5) of the aggregate. In all concrete compositions, a consistent ratio of fine-to-coarse aggregate (0.40 and 0.60, respectively) was maintained, with a constant slump of 80 mm (plastic consistency). CN concretes utilized 50% crushed stone and 50% normal coarse concrete aggregate. Concrete mixture ratios were determined following the ACI 211 principle (Committee&211, 1983). Following the preparation of fresh concrete mixtures based on the properties outlined in Tables 2 and 3, as well as the mixture ratios specified in Table 4 for the impact resistance experiment, the mixtures underwent compaction within cure molds utilizing a vibrator according to TS 3068 (TS 3068 ISO, 2736–2 1999) until reaching the designated experiment age. Subsequently, the cured concrete samples were safeguarded in an environment with 90% relative humidity and a temperature set at 23 ± 2 °C before being transferred to a water tank for the curing process. Concrete samples were kept in this position for 24 h and the impact application was launched after the samples completed their 28th day and the 48-h natural drying. Concrete samples at 30 °C were prepared in the drying oven and the concrete samples at 0 °C and − 25 °C in two deep freezers (no frost). The airborne freezing temperature was (0 ± 2 and − 25 ± 2 °C after the completion of the 28th day and 23 ± 2 °C at the end of the dissolution temperature. The concrete patterns underwent impact experiments following a total of 150 h of freezing–thawing conditions, comprising 100 h of freezing and 50 h of thawing. The impact experiment apparatus, with a consistent weight of 13.8 kg, utilized a free fall from distances of 25 cm and 30 cm. An ultrasonic test device was employed to assess potential changes in the internal structure and strength of the concrete before and after impact. Through this device, ultrasonic waves were directed into the concrete samples, and their pulse transmission periods were recorded. This method considered the "B" curve derived from the granulometry

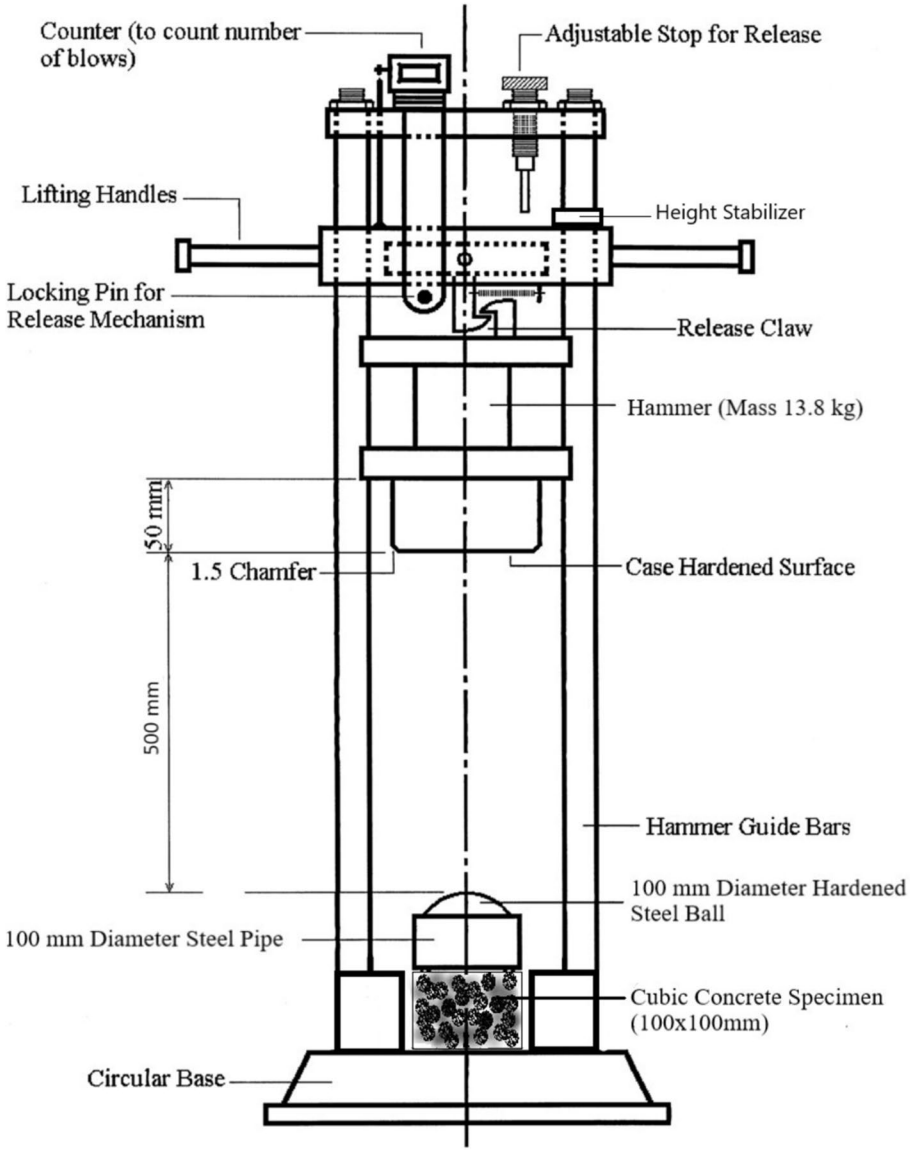

Fig. 4 Test equipment for impact resistance (Eren et al., 1999)

curve in TS 706 EN12620 + A1 with a 31.5 mm D_{max}. Pre-testing mixtures, prepared in line with the proportions in Table 4, were examined at the 28-day trial stage. Initially, weight (g) was measured, followed by determining pulse transmission velocity (UPTV) in km/s through the ultrasonic test. Later, pressure press and pressure resistance values were identified in MPa (Ekinci, 1995). Figs. 1 and 2 illustrate curves formed based on the acquired results. This curve was utilized to convert UPTV (Fig. 3) into equivalent cube compressive strength (ECCS) during consecutive impact applications. Free impacts were then administered, and measurements were taken for pre-experiment weight, weight loss, and pre-/after-experiment UPTV. The consecutive impact applications continued until fracture occurred on the lateral surfaces of the concrete samples. The latest weight, weight loss, and UPTV were determined after each consecutive impact, and the subsequent changes were analyzed to the curve derived from pre-testing mixtures (Cao et al., 2021; Committee&211, 1983; El-Hawary et al., 2021; Lee et al., 2021; Saberian March, 2021; Zebari et al., 2017). Compressive strength tests were conducted on concrete samples that were 28 days old according to the guidelines stated in TSEN 13791 (En&, 13791, 2010).

Concrete impact tests were carried out on 100 mm × 100 mm × 100 mm cubes. A drop weight type impact

Fig. 5 Some images of UPTV, compressive strength, and impact resistance tests

Table 5 Consistency and compressive strength experiment results

Concretes	Consistency experiment		28-day compressive strength (MPa)		
	Slump (mm)	W/C ratio that enables slump	Concretes at + 30 °C	Concretes at ± 0 °C	Concretes at −25 °C
N16	80	0.55	30.6	25.0	23.5
N31.5	80	0.51	36.6	32.6	24.6
C16	80	0.55	33.8	30.3	28.9
C31.5	80	0.51	48.8	38.4	33.1
CN16	80	0.55	41.9	36.8	30.9
CN31.5	80	0.51	42.8	37.3	33.0

testing device has been developed by modifying an aggregate impact testing machine by BS 812: Part 112 Method for Determination of Aggregate Impact Value. This device is a combination of aggregate impact tester and drop weight type testing apparatus recommended by ACI Committee 544 (Committee&544, 1988). This combination is shown in Fig. 4. Charpy impact testing, Izod impact testing, and drop weight testing are the most commonly used methods for determining the impact strength of concrete (Abbass et al., 2023; Abid et al., 2022; Alaloul et al., 2020; Costa et al., 2020; Eren et al., 1999; Haruna et al., 2021; Moein et al., 2023; Rahmati et al., 2023; Reis et al., 2021; Taghipoor & Sadeghian, 2022; Thomas & Sorensen, 2018). ANOVA analyses were conducted using the SPSS-21 package to assess the compressive strength, UPVT, impact strength, and freeze–thaw outcomes of concrete. During the impact test, a weight of 13.8 kg was dropped from two different heights, 25 cm and 30 cm, respectively. The concrete was exposed to approximately 9 Joule of energy for each drop from a height of 25 cm and 10Joule for each drop from a height of 30 cm. It was not possible to conduct an experimental study to determine the strain rate in the samples during impact.

The use of the ultrasound method in determining the compressive strength of concrete dates back to the 1950s. In summary, one of the first users was researcher Whitehurst. It has not been demonstrated that there is a significant relationship between Whitehurst compressive strength and ultrasound propagation speed. This suggests that there is no single correlation between concrete compressive strength and ultrasound velocity. In 1967, researcher Galan conducted a regression analysis between concrete compressive strength and acoustic properties of concrete such as UPTV and damping

Table 6 Impact experiment results for h = 25 cm

Concretes	Concrete temperature (°C)	Consecutive impact count	Weight before impact (g)	Weight after impact (g)	Weight loss (g)	Before the impact UPTV (km/s)	After the impact UPTV (km/s)	ECCS (MPa)
N16	30 ± 2	9	7580	7500	80	2.60	2.36	27
	0 ± 2	8	7950	7855	95	2.10	2.06	24
	−25 ± 2	6	8010	7960	105	2.00	1.81	22
N31.5	30 ± 2	12	8290	8220	70	3.17	2.41	28
	0 ± 2	10	8430	8340	90	2.95	2.14	25
	−25 ± 2	8	8410	8310	100	2.18	1.90	23
C16	30 ± 2	14	8050	7945	105	4.10	3.59	40
	0 ± 2	13	8160	8000	160	3.80	2.31	27
	−25 ± 2	10	8170	7975	195	3.63	2.25	26
C31.5	30 ± 2	14	8070	7980	90	5.28	3.61	40
	0 ± 2	12	8190	8050	140	4.41	3.43	38
	−25 ± 2	11	8180	8005	175	4.06	3.36	37
CN16	30 ± 2	13	7980	7855	125	4.11	3.42	38
	0 ± 2	11	8670	8460	190	3.90	3.35	37
	−25 ± 2	10	8370	8165	205	3.45	3.25	36
CN31.5	30 ± 2	15	8090	7975	115	4.24	3.31	38
	0 ± 2	13	8230	8060	170	3.81	3.10	34
	−25 ± 2	10	8240	8055	185	3.50	3.05	35

Table 7 Impact experiment results for h = 30 cm

Concretes	Concrete temperature (°C)	Consecutive impact count	Weight before impact (g)	Weight after impact (g)	Weight loss (g)	Before the impact UPTV (km/s)	After the impact UPTV (km/s)	ECCS (MPa)
N16	30 ± 2	9	7850	7770	80	2.85	2.15	24
	0 ± 2	7	8120	8025	95	2.45	2.01	23
	−25 ± 2	6	8140	8035	105	2.08	1.65	20
N31.5	30 ± 2	12	8240	8170	70	4.20	2.40	28
	0 ± 2	11	8400	8310	90	3.05	1.78	23
	−25 ± 2	10	8440	8340	100	2.87	1.70	20
C16	30 ± 2	13	8050	7945	105	5.10	3.50	38
	0 ± 2	12	8340	8180	160	4.20	3.10	35
	−25 ± 2	10	8140	7945	195	4.00	2.60	30
C31.5	30 ± 2	14	8090	8000	90	4.32	3.52	38
	0 ± 2	12	8240	8100	140	3.63	3.05	35
	−25 ± 2	10	8250	8075	175	3.57	2.95	34
CN16	30 ± 2	12	7980	7855	125	4.15	3.30	37
	0 ± 2	12	8460	8270	190	4.14	3.25	37
	−25 ± 2	9	8240	8035	205	3.85	2.95	34
CN31.5	30 ± 2	14	8090	7975	115	4.20	3.00	34
	0 ± 2	12	8250	8080	170	3.51	2.62	31
	−25 ± 2	10	8220	8035	185	3.24	3.05	35

coefficient. In 1973, Rajagopalan and colleagues proposed correlations between UPTV and concrete compressive strength for certain typical mixtures. In 1990, Tharmaratram and Tan proposed an empirical equation for the relationship between UPTV and concrete compressive strength. In 2004, Demirboga et al. proposed

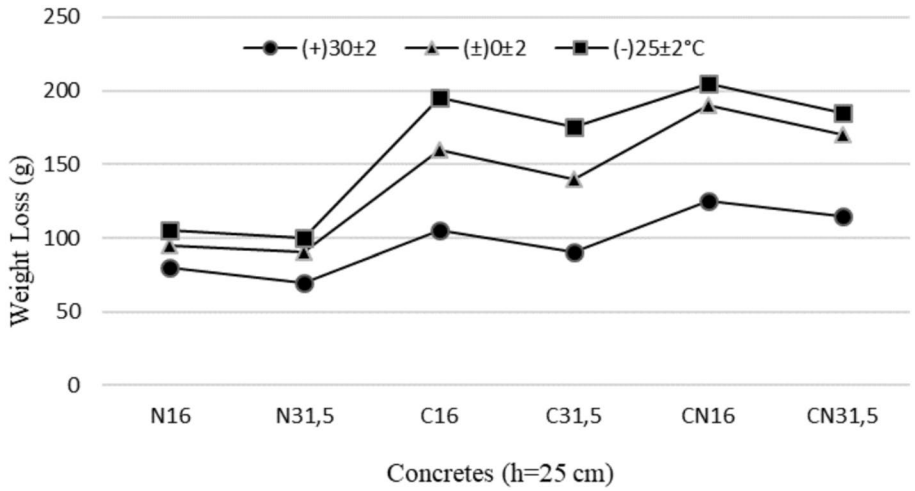

Fig. 6 Weight loss in concretes (h = 25 cm)

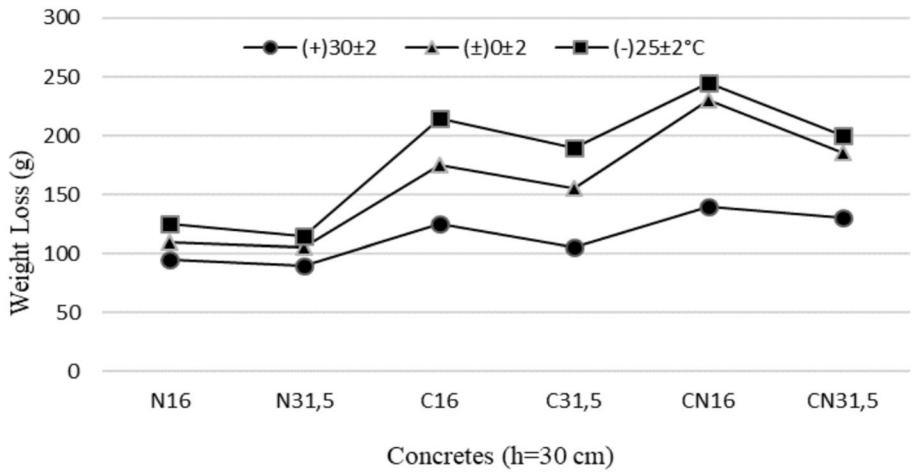

Fig. 7 Weight loss in concretes (h = 30 cm)

an exponential relationship between UPTV and compressive strength for mineral-added concretes. In 2009, Trtnik et al. They developed a widely used equation using the least squares method. In 2010, Mandandoust et al. suggested that for UPTV to be used, there should be a calibration curve for each material to be evaluated (Zebari et al., 2017). Some visuals of the experimental study process are given in Fig. 5. Nowadays, the formula UPTV = distance (kilometers) / time (seconds) is widely used.

4 Finding and Discussion

The outcomes derived from the experimental investigations are presented in a detailed manner in Tables 5, 6, and 7. The weights of the concrete specimens, invented for these experiments, range from 7580 to 8640 g. Following the consecutive impact tests, it was observed that N31.5 concrete exhibited minimal weight loss (70 g), while CN16 concrete proven the highest weight loss (205 g). Notably, the N16 concretes experienced structural disintegration after undergoing 6 successive impacts, whereas the CN31.5 concretes sustained structural integrity up to 15 consecutive impacts. Furthermore, concrete incorporating crushed-stone aggregate displayed elevated compressive strength values in comparison to concrete utilizing normal aggregate. The experimental protocol did not impose a uniform count of consecutive impacts on the concrete specimens. Instead, the study extended the sequence until the smooth surface area of the UPTV device, employed for measurements, was compromised. Consequently, a specialized analysis of the UPTV values was left out due to the varying number of consecutive pulses. However, it is noteworthy

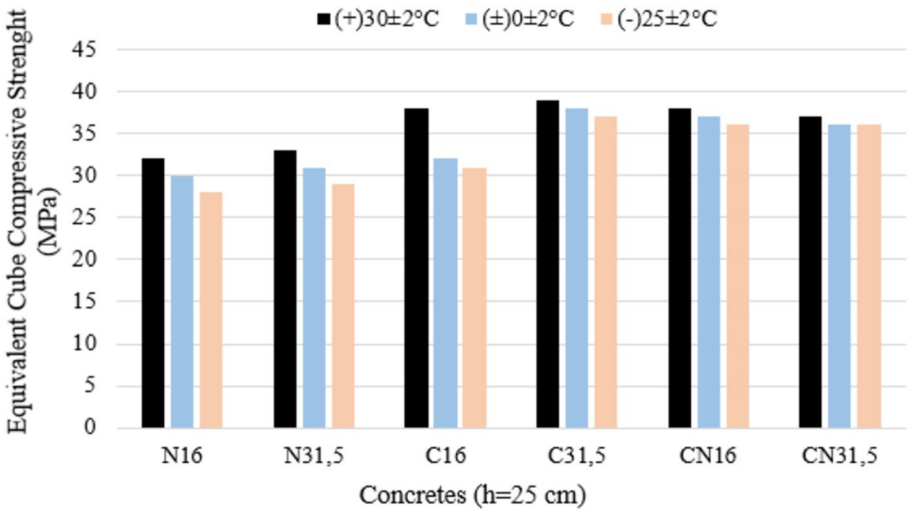

Fig. 8 Equivalent cube compressive strength (h = 25 cm)

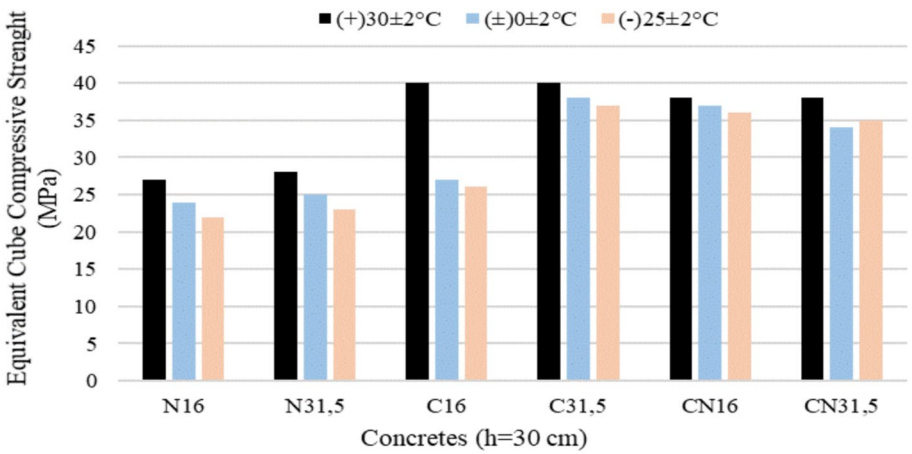

Fig. 9 Equivalent cube compressive strength (h = 30 cm)

that the frequency of consecutive impacts diminished with decreasing concrete temperature. For instance, in the case of N16 concrete at 30 ± 2 °C, the UPTV value decreased from 2.60 km/s to 2.36 km/s after 9 consecutive impacts with an impact height (h) of 25 cm. Similarly, when the UPTV value of N16 concrete was assessed at − 25 ± 2 °C following 6 consecutive impacts with an impact height of 25 cm, it decreased from 2.00 km/s to 1.81 km/s. Concurrently, a reduction in temperature corresponded to a decline in both the number of impacts and the compressive strength of the concrete. Fig. 6 shows the change in weight loss at a height of h = 25 cm.

In Table 7 the case of N16 concrete at 30 ± 2 °C, the UPTV value decreased from 2.85 km/s to 2.15 km/s after 9 consecutive impacts with an impact height (h) of 30 cm. Similarly, when the UPTV value of N16 concrete was assessed at − 25 ± 2 °C following 7 consecutive impacts with an impact height of 30 cm, it decreased from 2.08 km/s to 1.65 km/s. Concurrently, a reduction in temperature corresponded to a decrease in both the number of impacts and the compressive strength of the concrete. Following the consecutive impact tests, it was observed that N31.5 concrete exhibited minimal weight loss (70 g), while CN16 concrete demonstrated the highest weight loss (205 g). Notably, the N16 concretes experienced structural disintegration after undergoing 6 consecutive impacts, whereas the CN31.5 concretes sustained structural integrity for up to 14 consecutive impacts. Furthermore, concrete incorporating crushed-stone aggregate displayed elevated compressive strength

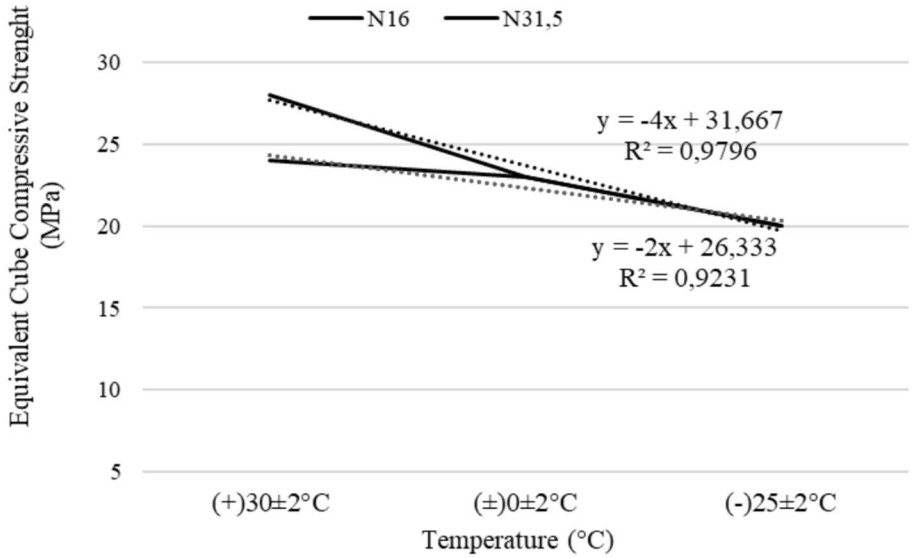

Fig. 10 ECCS change of the normal aggregated concretes at different temperatures

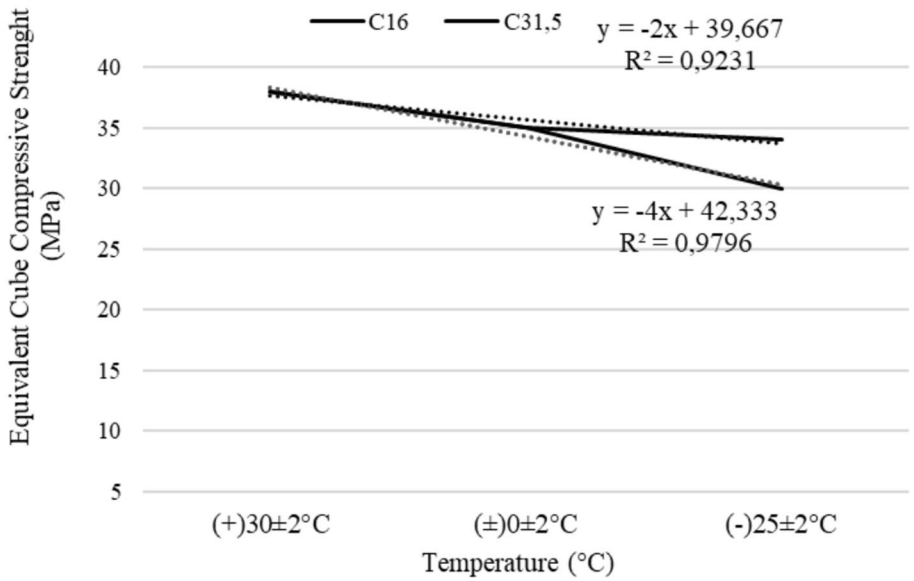

Fig. 11 ECCS change of the crushed-stone aggregated concretes at different temperatures

values in comparison to concrete utilizing normal aggregate. Fig. 7 shows the change in weight loss at a height of h = 30 cm. The compressive strength results of concrete are given in Figs. 8 and 9, and the ECCS changes of normal and crushed-stone aggregate concrete at different temperatures are given in Figs. 10 and 11. The ECCS change of 50% normal and 50% crushed-stone aggregate concretes at different temperatures is given in Fig. 12.

4.1 General Evaluation of Compressive Strength Results

The compressive strength of concrete is influenced by the size, shape, and fineness modulus of the particles. As indicated in Tables 5, 6, and 7, the outcomes for compressive strength exhibit a direct relationship with the aggregate size. Simultaneously, a reduction in ambient temperature corresponds to a decrease in compressive strength values. This comprehensive finding suggests that opting for a larger aggregate diameter is a valid approach for the production of concrete with enhanced strength.

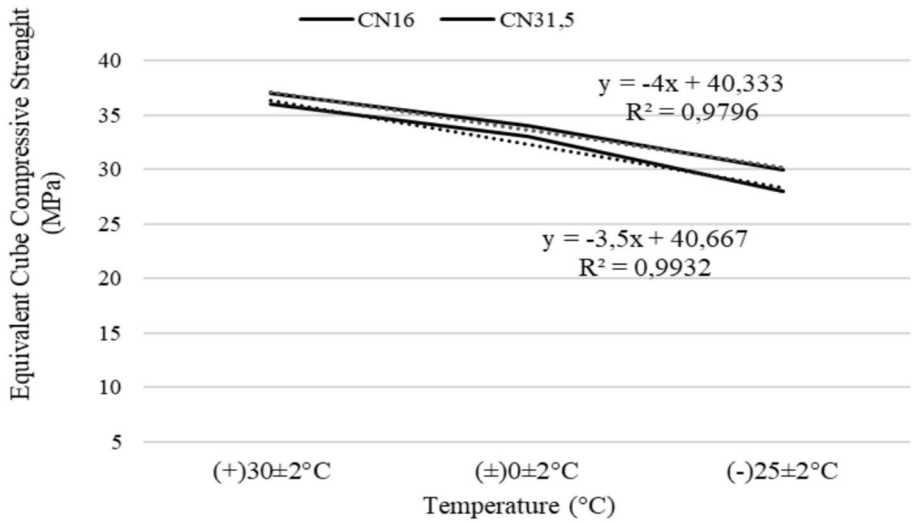

Fig. 12 ECCS change of the 50% normal and 50% crushed-stone aggregated concretes at different temperatures

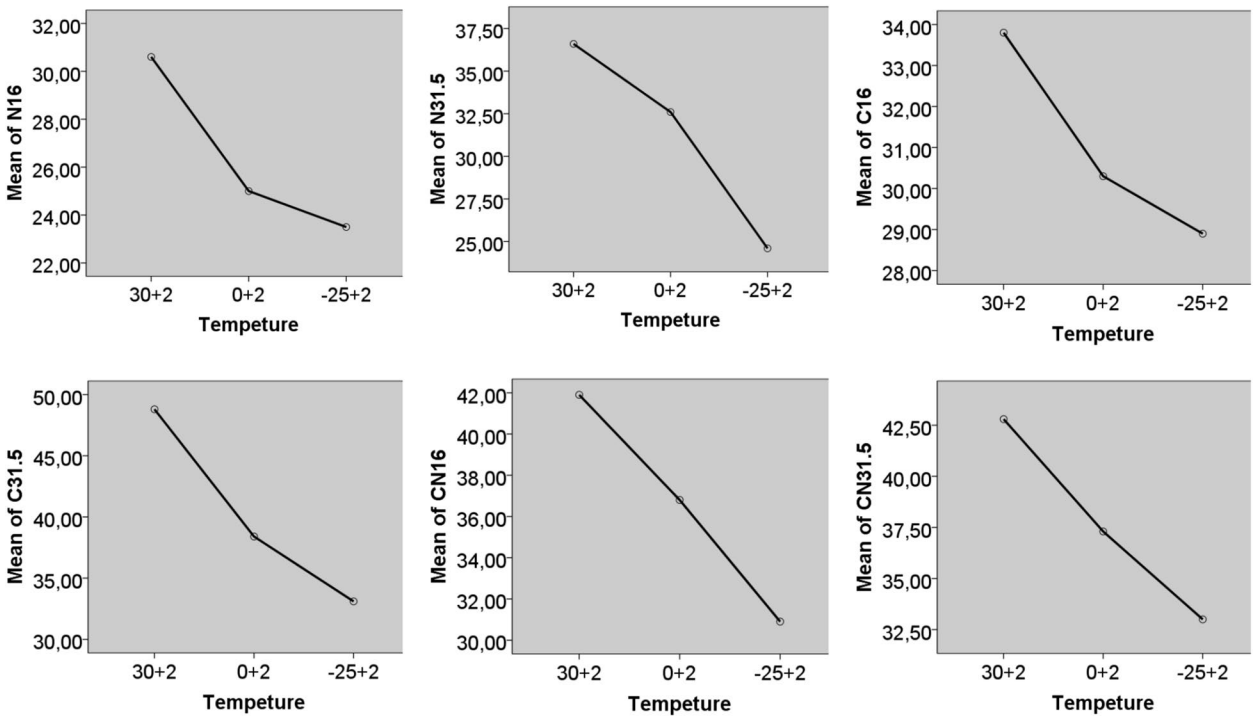

Fig. 13 Mean plots of compressive strength values of concrete

Table 8 Results of ANOVA for compressive strength values

Source	DF	SS	MS	F	P
Concretes	6	395.6	79.1	2.70	0.074
Error	12	351.9	29.3		
S = 5.415 R-Sq = 52.93% R-Sq(adj) = 33.31%					

Table 9 Results of ANOVA for UPTV values (h = 25 cm)

Source	DF	SS	MS	F	P
Concretes	6	4.825	0.603	2.56	0.092
Error	9	2.124	0.236		

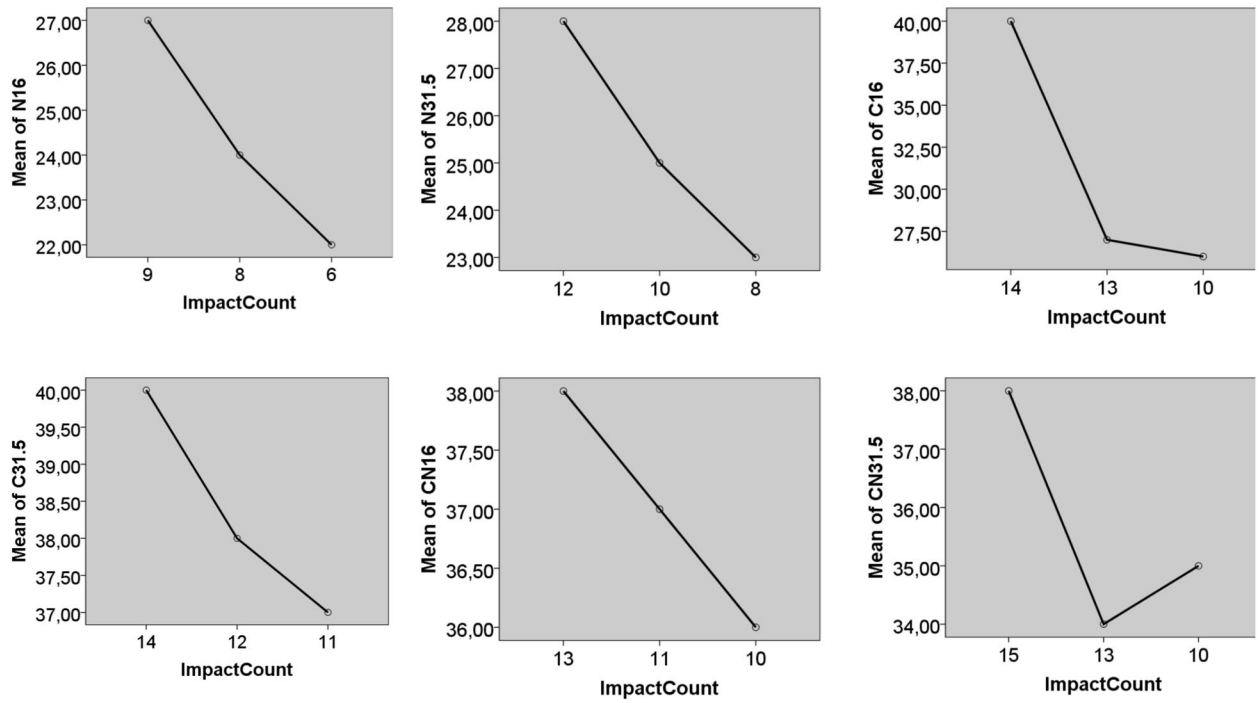

Fig. 14 Mean plots of UPTV of concrete (h = 25 cm)

Table 10 Results of ANOVA for UPTV values (h = 30 cm)

Source	DF	SS	MS	F	P
Concretes	6	3.178	0.454	1.35	0.323
Error	10	3.371	0.337		
S = 0.5806 R-Sq = 48.52% R-Sq(adj) = 12.49%					

For example, in Fig. 13, sample N16 is seen to be 30.6 MPa at 30 ± 2 °C, 25.0 MPa at 0 ± 2 °C, and 23.5 MPa at − 25 ± 2 °C. The significance value given in Table 8 is greater than P > 0.05. A large value indicates that there is a homogeneous distribution among the variances. This means that as the temperature decreases, the strength values also decrease similarly between the samples.

4.2 General Evaluation of UPTV Results

The investigation has elucidated the significance of the water/cement ratio and compactness in determining the compressive strength of concrete, emphasizing the critical role of meticulous bottling and proper placement of fresh concrete into the mold. Tables 6 and 7 reveal a consistent trend where UPTV values exhibit a decline with an increase in impact height and a decrease in surroundings temperature. This decline is attributed to the development of internal cracks within the concrete structure following impact. Moreover, it is observed that as the aggregate diameter in concrete expands, UPTV values also register an increase. The significance value given in Table 9 is greater than P > 0.05. A large value indicates that there is a homogeneous distribution among the variances. As the number of impacts decreases, UPVT values also decrease similarly. When the C16 example in Fig. 14 is examined, it is seen that the UPVT value is 3.59 km/s after 14 impacts and 2.25 km/s after 10 impacts. That is, as the number of pulses decreases, the UPVT value also decreases.

The significance value given in Table 10 is greater than P > 0.05. A large value indicates that there is a homogeneous distribution among the variances. As the number of impacts decreases, UPVT values also decrease similarly. When the C31.5 example in Fig. 15 is examined, it is seen that the UPVT value is 3.52 km/s after 14 impacts and 2.95 km/s after 10 impacts. That is, as the number of impacts decreases, the UPVT value also decreases.

4.3 General Evaluation of Impact Resistance Results

The significance of ambient temperature and the distance of impact application in influencing the compressive strength of concrete has been recognized. As depicted in Tables 6 and 7, concrete exhibits earlier degradation with an increase in impact application and a decrease in ambient temperature. This observation is attributed to the adverse impact of freezing on the internal structure of the concrete at lower temperatures. The weight losses observed in concrete further validate this phenomenon.

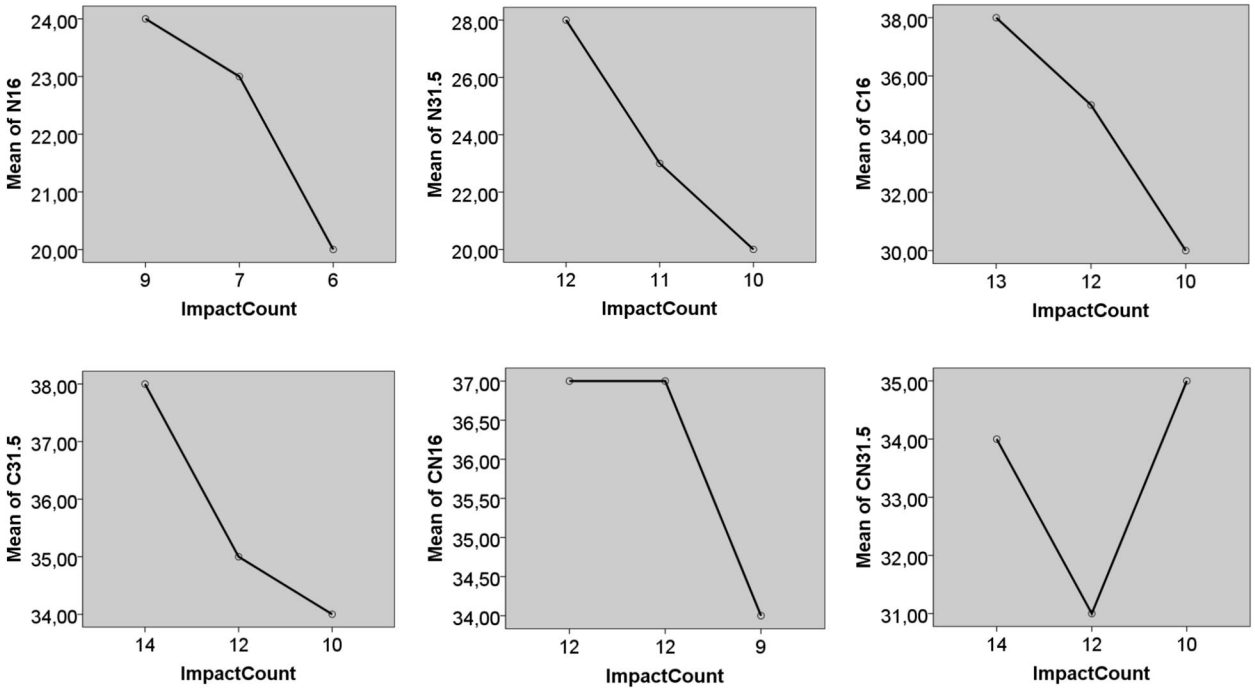

Fig. 15 Mean plots of UPTV of concrete (h = 30 cm)

Table 11 Results of ANOVA for impact resistance values (h = 25 cm)

Source	DF	SS	MS	F	P
Concretes	6	534.5	106.9	7.64	0.002
Error	12	168.0	14.0		
S = 3.742 R-Sq = 76.09% R-Sq(adj) = 66.12%					

The significance value given in Table 11 is less than P > 0.05. The value of 0.002 illustrated that there was a significant difference between concretes. In other words, as weight loss increases, the ECCS value of concrete decreases. When the CN31.5 example in Fig. 16 is examined, it is seen that it gets the value of 38 MPa at 115 g weight loss and 35 MPa value at 185 g weight loss. In other words, when weight loss increases, the ECCS value decreases.

The significance value given in Table 12 is less than P > 0.05. The value of 0.001 showed that there was a significant difference between concretes. In other words, as weight loss increases, the ECCS value of concrete decreases. When the C31.5 example in Fig. 17 is examined, it is seen that it gets the value of 38 MPa at 90 g weight loss and 34 MPa value at 175 g weight loss. In other words, when weight loss increases, the ECCS value decreases.

4.4 General Evaluation of Freeze–Thaw Results

It has been established that the periodic process of freezing and thawing plays a crucial role in influencing the compressive strength of concrete. As evidenced in Tables 6 and 7, the enlargement of aggregate diameter in concrete leads to a reduction in weight losses caused by freezing–thawing, an increase in compressive strength values, and the potential to obtain concrete structures that exhibit greater resistance to successive impacts. The overarching conclusions presented align notably with existing research exploring the impact of freeze–thaw cycles on compressive strength and the correlation between aggregate diameter and compressive strength (Cao et al., 2021; Ekinci, 1995; El-Hawary et al., 2021; Karakurt & Bayazit, 2015; Lee et al., 2021; Saberian March, 2021).

As a result (Table 13), in the study conducted by Ekinci in 1995 on the use of silica fumes in concrete, with the freeze–thaw UPVT value; With the weight loss, deformation and compressive strength values in the study conducted by Karakurt and Bayazit in 2015 in which the freeze–thaw resistance of air-entrained and non-air-entrained normal strength concretes was investigated. In the study conducted by Lee, Park, Kim, and Kang in 2021, rubber crumb addition was related to the development of compressive strength of concrete and its behavior against freezing and thawing; Freeze–thaw cycles conducted by Cao, Liu, Zhou, Ge, and Zhang in 2021, axial tensile

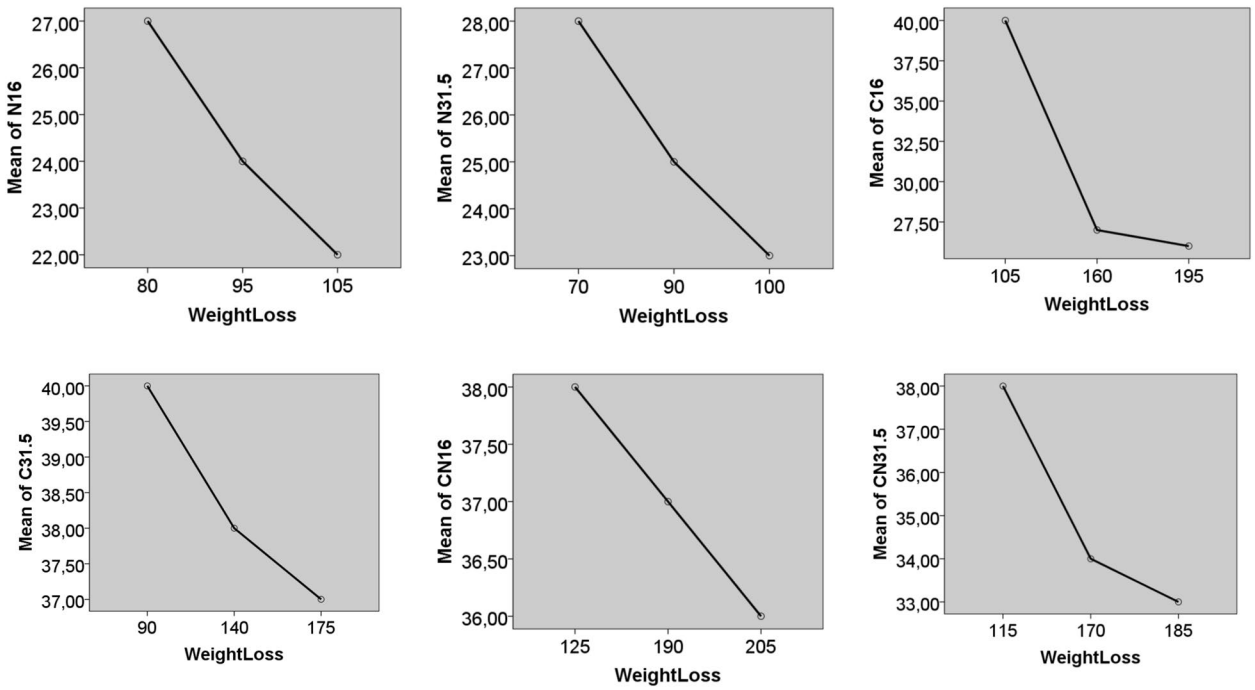

Fig. 16 Mean plots of impact resistance values of concrete (h = 25 cm)

Table 12 Results of ANOVA for impact resistance values (h = 30 cm)

Source	DF	SS	MS	F	P
Concretes	6	576.44	115.29	14.21	0.001
Error	12	97.33	8.11		
S = 2.848 R-Sq = 85.55% R-Sq(adj) = 79.53%					

and axial compressive strengths and deformation behaviors of carbonized concrete; in the study conducted by El-Hawary, Al-Yaqout, and Elsayed in 2021, where the resistance of concretes with partial replacement of recycled coarse aggregate (RAC) and cement with mineral slag was investigated against freeze–thaw cycles, it can be said that it is agreeable with compressive strength, mass loss and ultrasonic pulse velocity behaviors.

5 Conclusions

The ultrasonic pulse transmission velocity serves as a valuable indicator for determining the relative attrition of concrete samples subjected to pressure and consecutive impact experiments under varying temperature conditions. Analysis of Table 5 reveals that the size and shape of aggregates in concrete contribute positively to both pressure and impact resistance. When concretes are exposed to lower temperatures and consecutive impacts, a notable reduction in compressive strength is evident, as illustrated in Tables 5, 6, Figs. 8, and 9. In concretes containing normal aggregates, the majority of the fractures result from aggregate separation from their base in response to the pressure and consecutive impact experiment. On the other hand, concretes with both normal and crushed stones exhibit a combination of normal aggregates separating from the base and breaking, particularly in the middle, in the case of crushed stones. The usage of crushed stones in concretes, as indicated in Tables 5, 6, and 7, enhances their ability to resist consecutive impacts. However, a decrease in the Equivalent Cube Compressive Strength (ECCS) value is observed post-breakage (Figs. 10, 11 and 12). Furthermore, the R2 values for the concretes exceed 90%, indicating a strong correlation between the experimentally obtained results and the suggested regression equations. Selecting aggregates with varying grain sizes is a wise choice for producing concrete of superior quality. The study demonstrates that selecting qualified aggregates with maximum particle sizes enhances concrete resistance to damage from factors such as impact and freeze–thaw. Examining Table 14 reveals that normal concrete exhibited the highest percentage change in compressive strength ($\bar{x} = 140$), while crushed-stone concrete displayed the lowest percentage change ($\bar{x} = 132$). Crushed stone + normal aggregate concrete falls in between, with a percentage change in compressive strength of $\bar{x} = 133$. These findings suggest that incorporating crushed stone in concrete intended

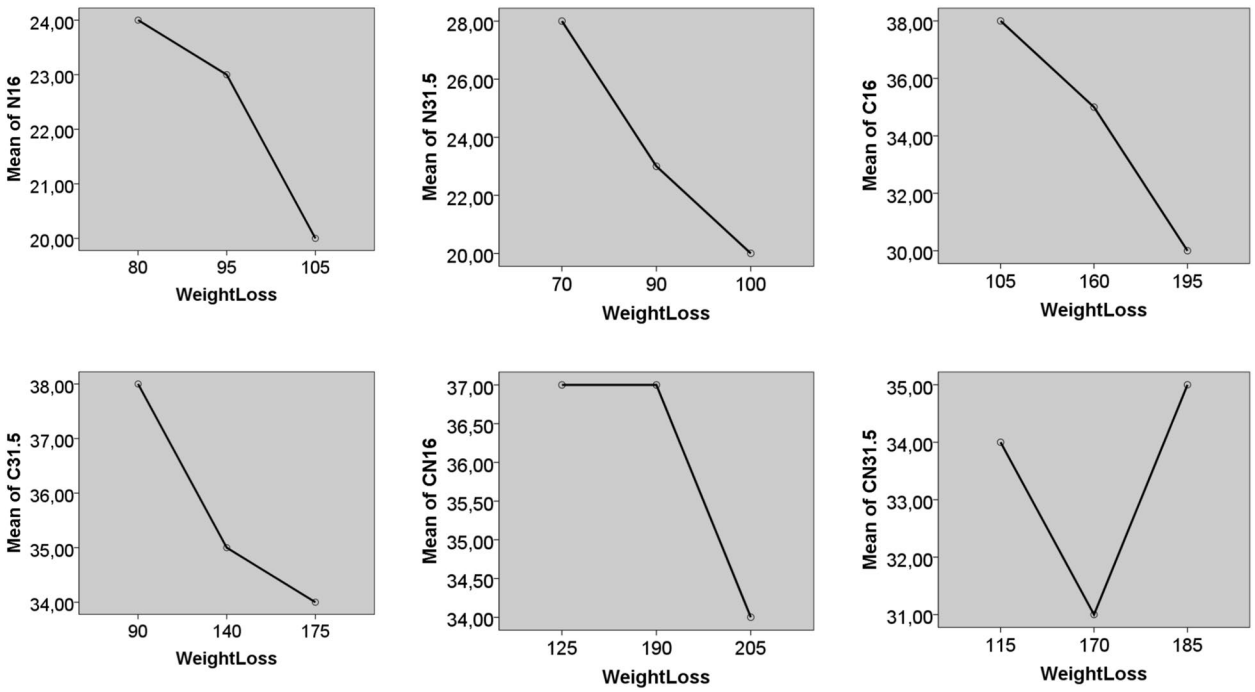

Fig. 17 Mean plots of impact resistance values of concrete (h = 30 cm)

Table 13 General comparison of freeze–thaw experiment

Previous studies and their authors				General comparison			
				1	2	3	4
Ekinci, 1995)	Ekinci, 1995			+	+	+	+
Saberian March, 2021)	Saberian and Li, 2021			±	+	±	+
Lee et al., 2021)	Lee, Park, Kim and Kang, 2021			±	+	±	+
Cao et al., 2021)	Cao, Liu, Zhou, Ge, and Zhang, 2021			±	+	+	+
El-Hawary et al., 2021)	El-Hawary, Al-Yaqout and Elsayed, 2021			+	±	±	+
Fédération internationale du béton – FIB. fib Bulletin 38: Fire design of concrete structures – materials, 2007)	Karakurt and Bayazit, 2015			+	±	+	+
Note	1	Weight loss	2	Freeze–thaw process			
	3	Shapeshifting	4	Compressive strength			
	(+)	Compatible	(±)	Partially compatible			

Table 14 Change in compressive strength values of concretes according to ambient temperature

Concretes	Concretes at + 30 °C ECCS (MPa)	Concretes at 0 °C ECCS (MPa)	Concretes at −25 °C ECCS (MPa)	% Change of ECCS (−25 °C and + 30 °C)	x̄
N16	30.6	25.0	23.5	130	140
N31.5	36.6	32.6	24.6	149	
C16	33.8	30.3	28.9	117	132
C31.5	48.8	38.4	33.1	147	
CN16	41.9	36.8	30.9	136	133
CN31.5	42.8	37.3	33.0	130	

for areas prone to freezing and thawing is a more suitable choice.

Consequently, based on the trends depicted in Figs. 8, 9, and 10, it has been concluded that the usage of crushed stones with high D_{max} in concrete for locations subjected to consecutive impact effects in zero or lower atmospheric conditions would be advantageous.

Abbreviations

N16	Normal aggregated concrete with 16 mm D_{max}
C16	Crushed-stone aggregated concrete with 16 mm D_{max}
CN16	50% Crushed stone coarse, 50% normal aggregated concrete with 16 mm D_{max} and aggregate
UPTV	Ultrasonic pulse transmission velocity (km/s)
ECCS	Equivalent cube compressive strength (MPa)
D_{max}	Aggregate size (mm)
SSD	Saturated surface-dry weight of the aggregate (g/cm^3)
W/C	Water/cement
BPC	Blended Portland cement

Acknowledgements
Not applicable.

Author contributions
CEE: conducted the experimental study, analyzed the test results and presented the manuscript. BE: participated in the experimental studies, participated in the analysis of the test results, and prepared the manuscript.

Funding
No financial support was received for this study.

Availability of data and materials
The data that support the findings of this study are available from the corresponding author, upon reasonable request.

Declarations

Ethics approval and consent to participate
All authors of the manuscript confirm ethical approval and consent to participate following the Journal's policies.

Consent for publication
All authors of the manuscript agree on the publication of this work in the *International Journal of Concrete Structures and Materials*.

Competing interests
The authors report no competing interests.

Received: 15 February 2024 Accepted: 20 May 2024
Published online: 27 March 2025

References

Abbass, A. A., Abid, S. R., Abed, A. I., & Ali, S. H. (2023). Experimental and statistical study of the effect of steel fibers and design strength on the variability in repeated impact test results. *Fibers., 11*(1), 4. https://doi.org/10.3390/fib11010004

Abid, S. R., Murali, G., Ahmad, J., Al-Ghasham, T. S., & Vatin, N. I. (2022). Repeated drop-weight impact testing of fibrous concrete: State-of-the-art literature review, analysis of results variation and test improvement suggestions. *Materials, 15*(11), 3948. https://doi.org/10.3390/ma15113948

ACI Committee 544. (1988). Design considerations for steel fiber reinforced concrete. *ACI Structural Journal, Committee Report, 85*, 563–580.

Alaloul, W. S., John, V. O., & Musarat, M. A. (2020). Mechanical and thermal properties of interlocking bricks utilizing wasted polyethylene terephthalate. *Int J Concr Struct Mater, 14*, 24. https://doi.org/10.1186/s40069-020-00399-9

Alwesabi, E. A., Abu Bakar, B. H., Alshaikh, I. M. H., & Md Akil, H. (2020). Impact resistance of plain and rubberized concrete containing steel and polypropylene hybrid fiber. *Materials Today Communications, 25*, 101640. https://doi.org/10.1016/j.mtcomm.2020.101640

Cantwell, W. J., & Morton, M. (1991). The impact resistance of composite materials- A review. *Composites, 22*(5), 347–362.

Cao, D., Liu, J., Zhou, Y., Ge, W., & Xin Zhang, X. (2021). Experimental study on the effect of freeze–thaw cycles on axial tension and compression performance of concrete after complete carbonization. *Advances in Civil Engineering, 2021*, 8111436. https://doi.org/10.1155/2021/8111436

ACI Committee 211. (1983). Standard practice for selecting proportions for normal, heavyweight and mass concrete. aci manual of concrete practice, part: 1, American Concrete Institute, Detroit, Michigan.

Costa, U. O., Cassiano Nascimento, L. F., Magalhães Garcia, J., Almeida Bezerra, W. B., & Monteiro, S. N. (2020). Evaluation of Izod impact and bend properties of epoxy composites reinforced with mallow fibers. *Journal of Materials Research and Technology, 9*(1), 373–382. https://doi.org/10.1016/j.jmrt.2019.10.066

Dok, G., Caglar, N., & Ilki, A. (2020). Yilmaz C (2020) Effect of impact loading on residual flexural capacity of high-strength reinforced concrete beams. *Structures, 27*, 2466–2480. https://doi.org/10.1016/j.istruc.2020.08.054

Drathi, R. (2015). Impact resistance of concrete structures. *Mathematical Problems in Engineering, 2015*, 494617. https://doi.org/10.1155/2015/494617

Ekinci, C. E. (1995). Antalya etibank elektrometalurji işletmesi silis dumanlarının çimento ve betonda katkı maddesi olarak değerlendirilmesi (Doktora Tezi). Fırat Üniversitesi Fen Bilimleri Enstitüsü (In Turkish).

Ekinci, C.E. (2024). Bordo Kitap: Mimar ve Mühendisin Insaat El Kitabi (In Turkish, 13th ed.) (Maroon Book: Architect and Engineer's Construction Handbook), Ankara: Data Publications, ISBN: 978–625–7951–13–5.). https://web.archive.org/web/20241228115536/https://www.datayayinlari.com/urun/bordo-kitap-mimar-ve-muhendisin-insaat-el-kitabi.

Ekinci, C. E. (2024). Yapı (In Turkish, 2nd ed.) (Construction). Ankara: Data Publications. ISBN: 978–625–7552–83-7. https://web.archive.org/web/20241228115124/https://www.datayayinlari.com/urun/yapi-cevdet-emin-ekinci.

Ekinci, C. E. (2006). The calculation methods of compound of concrete and a novel calculation method. *E-Journal of New World Sciences Academy, 1*(1), 1–12. https://web.archive.org/web/20241228114944/https://dergipark.org.tr/en/download/article-file/187430.

Ekinci, C. E., & Kelesoglu, O. (2014). A study on occupancy and compressive strength of concrete with produced injection method. *Advances in Materials Sciences and Engineering*. https://doi.org/10.1155/2014/241613

El-Hawary, M., Al-Yaqout, A., & Elsayed, K. (2021). Freezing and thawing cycles: Effect on recycled aggregate concrete including slag. *International Journal of Sustainable Engineering, 14*(4), 800–808. https://doi.org/10.1080/19397038.2021.1886374

Eren, O., Marar, K., & Celik, T. (1999). Effects of silica fume and steel fibers on some mechanical properties of high-strength fiber-reinforced concrete. *Journal of Testing and Evaluation*. https://doi.org/10.1520/JTE12166J

Etman, Z. A., & Ahmed, T. I. (2018). Effect of freezing-thawing on concrete behavior. *Challenge Journal of Concrete Research Letters, 9*(1), 21–36. https://doi.org/10.20528/cjcrl.2018.01.003

Fabbro, S., Araujo, L. M., Engel, J., Kondratiuk, J., Kuffa, M., & Wegener, K. (2021). Abrasive and adhesive wear behaviour of metallic bonds in a synthetic slurry test for wear prediction in reinforced concrete. *Wear, 476*, 203690. https://doi.org/10.1016/j.wear.2021.203690

Fédération internationale du béton – FIB. fib Bulletin 38: Fire design of concrete structures – materials, structures and modelling, 2007, 106 p.

Fédération internationale du béton – FIB. fib Bulletin 46: Fire design of concrete structures-structural behaviour and assessment, 2008, 214 p.

Georgali, B., & Tsakiridis, P. E. (2005). Microstructure of fire damaged concrete A case study. *Cement and Concrete Composites, 27*(2), 255–259.
Guo, Z., & Shi, X. (2011). *Experiment and calculation of reinforced concrete at elevated temperatures*. Waltham: Butterworth-Heinemann.
Hager, I. (2013a). Behaviour of cement concrete at high temperature. *Bulletin of the Polish Academy of Sciences: Technical Sciences, 61*(1), 1–10.
Hager, I. (2013b). Colour change in heated concrete. *Fire Technology, 50*(4), 945–958.
Haruna, S. I., Zhu, H., Jiang, W., & Shao, J. (2021). Evaluation of impact resistance properties of polyurethane-based polymer concrete for the repair of runway subjected to repeated drop-weight impact test. *Construction and Building Materials, 309*, 125152. https://doi.org/10.1016/j.conbuildmat.2021.125152
Hourt, G. A. (2000). Effect of fire on concrete and concrete structures. *Progress in Structural Engineering and Materials, 2*(4), 429–447.
Karakurt, C., & Bayazit, Y. (2015). Freeze–thaw resistance of normal and high strength concretes produced with fly ash and silica fume. *Advances in Materials Science and Engineering, 2015*, 830984. https://doi.org/10.1155/2015/830984
Lee, S. T., Park, S. H., Kim, D. G., & Kang, J. M. (2021). Effect of freeze–thaw cycles on the performance of concrete containing water-cooled and air-cooled slag. *Applied Sciences, 11*, 7291. https://doi.org/10.3390/app11167291
Li, T., Liu, X., Wei, Z., Zhao, Y., & Yan, D. (2021). Study on the wear-resistant mechanism of concrete based on wear theory. *Construction and Building Materials, 271*, 121594. https://doi.org/10.1016/j.conbuildmat.2020.121594
Liu, D., Tu, Y., Sas, G., & Elfgren, L. (2021). Freeze–thaw damage evaluation and model creation for concrete exposed to freeze–thaw cycles at early-age. *Construction and Building Materials*. https://doi.org/10.1016/j.conbuildmat.2021.125352
Luo, S., Bai, T., Guo, M., Wei, Y., & Ma, W. (2022). Impact of freeze–thaw cycles on the long-term performance of concrete pavement and related improvement measures: A review. *Materials, 15*(13), 4568. https://doi.org/10.3390/ma15134568
Moein, M. M., Saradar, A., Rahmati, K., Rezakhani, Y., Ashkan, S. E., & Moses Karakouzian, M. (2023). Reliability analysis and experimental investigation of impact resistance of concrete reinforced with polyolefin fiber in different shapes, lengths, and doses. *Journal of Building Engineering, 69*, 106262. https://doi.org/10.1016/j.jobe.2023.106262
Moein, M. M., Saradar, A., Rahmati, K., Shirkouh, A. H., Sadrinejad, I., Aramali, V., & Moses Karakouzian, M. (2022). Investigation of impact resistance of high-strength Portland cement concrete containing steel fiber. *Materials, 15*(20), 7157. https://doi.org/10.3390/ma15207157
Niță, A., Petrescu, M. G., Dumitru, T., Burlacu, A., Tănase, M., Laudacescu, E., & Ramadan, I. (2023). Experimental research on the wear behavior of materials used in the manufacture of components for cement concrete mixers. *Materials, 16*(6), 2326. https://doi.org/10.3390/ma16062326
Oltulu, M., & Altun, M. G. (2018). The drop weight test method to determine impact strength of concrete and a review of research. *GÜFBED/GUSTIJ, 8*(1), 155–163. https://doi.org/10.17714/gumusfenbil.318540.
Pham, T. M., Chen, W., Khan, A. M., Hao, H., Elchalakani, M., & Tran, T. M. (2020). Dynamic compressive properties of lightweight rubberized concrete. *Construction and Building Materials, 238*, 117705. https://doi.org/10.1016/j.conbuildmat.2019.117705
Rafieizonooz, M., Khankhaje, E., & Rezania, S. (2020). Assessment of environmental and chemical properties of coal ashes including fly ash and bottom ash, and coal ash concrete. *Journal of Building Engineering, 49*, 104040. https://doi.org/10.1016/j.jobe.2022.104040
Raghav, M., Park, T., Yang, H.-M., Lee, S.-Y., Karthick, S., & Lee, H.-S. (2021). Review of the effects of supplementary cementitious materials and chemical additives on the physical, mechanical and durability properties of hydraulic concrete. *Materials., 14*(23), 7270. https://doi.org/10.3390/ma14237270
Rahmati, K., Saradar, A., Mohtasham, M. M., Sardrinejad, I., Bristow, J., Yavari, A., & Moses Karakouzian, M. (2023). Evaluation of engineered cementitious composites (ECC) containing polyvinyl alcohol (PVA) fibers under compressive, direct tensile, and drop-weight test. Multiscale and Multidiscip. *Modeling Experiments and Design, 6*, 147–164. https://doi.org/10.1007/s41939-022-00135-8
Reis, R. H. M., Garcia Filho, F. C., Nunes, L. F., Candido, V. S., Silva, A. C. R., & Monteiro, S. N. (2021). Impact resistance of epoxy composites reinforced with Amazon Guaruman fiber: A brief report. *Polymers, 13*(14), 2264. https://doi.org/10.3390/polym13142264
Saberian, M. (2021). Li J (2021) Effect of freeze–thaw cycles on the resilient moduli and unconfined compressive strength of rubberized recycled concrete aggregate as pavement base/subbase. *Transportation Geotechnics, 27*, 100477. https://doi.org/10.1016/j.trgeo.2020.100477
Saleem, M. A., Saleem, M. M., Ahmad, Z., & Hayat, Z. (2021). Predicting compressive strength of concrete using impact modulus of toughness. *Case Studies in Construction Materials, 14*, e00518. https://doi.org/10.1016/j.cscm.2021.e00518
Suryawanshi, N. T., Nayak, C. B., Thakare, S. B., & Kate, G. K. (2022). Optimization of self-cured high-strength concrete by experimental and grey taguchi modelling. *Iranian Journal of Science and Technology-Transactions of Civil Engineering, 46*(4), 4313–4326. https://doi.org/10.1007/s40996-022-00897-8
Taghipoor, H., & Sadeghian, A. (2022). Experimental investigation of single and hybrid-fiber reinforced concrete under drop weight test. *Structures, 43*, 1073–1083. https://doi.org/10.1016/j.istruc.2022.07.030
Thomas, R. J., & Sorensen, A. D. (2018). Charpy impact test methods for cementitious composites: Review and commentary. *ASTM International Journal Testing and Evaluation, 46*(6), 2422–2430. https://doi.org/10.1520/JTE20170057
TS 3068 ISO 2736–2 (1999) Concrete tests- test specimens- part 2: making and curing of test specimens for strength tests. Ankara: Turkish Standards Institute.
TS 706 EN 12620+A1 (2009) Aggregates for concrete. Ankara: Turkish Standards Institute.
TS 699 (2009) Natural building stones - methods of inspection and laboratory testing. Ankara: Turkish Standards Institute.
TS EN 13791 (2010) Test Method for concrete- obtaining samples and determination of compressive strength in hardened concrete in structures and components. Ankara: Turkish Standards Institute.
TS EN 197–1 (2012) Overall Cement Types - Part 1: Overall Cement Types-Composition, Properties and Eligibility Criteria's. Ankara: Turkish Standards Institute.
Wan, F., Jiang, Z., Tan, Q., & Cao, Y. (2016). Response of steel tube confined concrete targets to projectile impact. *International Journal of Impact Engineering, 94*, 50–59. https://doi.org/10.1016/j.ijimpeng.2016.03.012
Wang, R., Hu, Z., Li, Y., Wang, K., & Zhang, H. (2022). Review on the deterioration and approaches to enhance the durability of concrete in the freeze–thaw environment. *Construction and Building Materials, 321*, 126371. https://doi.org/10.1016/j.conbuildmat.2022.126371
Wang, R., Zhang, Q., & Li, Y. (2021). Deterioration of concrete under the coupling effects of freeze–thaw cycles and other actions: A review. *Construction and Building Materials, 319*, 126045. https://doi.org/10.1016/j.conbuildmat.2021.126045
Wang, Y., Huang, B., Mao, Z., Deng, M., & Cao, H. (2020). Effect of a boric acid corrosive environment on the microstructure and properties of concrete. *Materials., 13*(21), 5036. https://doi.org/10.3390/ma13215036
Wang, Y., Xie, M., & Zhang, Z. (2023). Mechanical properties and damage model of modified recycled concrete under freeze–thaw cycles. *Journal of Building Engineering, 78*, 107680. https://doi.org/10.1016/j.jobe.2023.107680.Wang(2023)
Warudkar, A., & Elavenil, S. (2020). A comprehensive review on abrasion resistance of concrete. *International Journal of Applied Science and Engineering, 17*(1), 29–43. https://doi.org/10.6703/IJASE.202003_17(1).029.
Wong, L. S. (2022). Durability performance of geopolymer concrete: A review. *Polymers, 14*(5), 868. https://doi.org/10.3390/polym140508682022
Ya Trofimov, B., Ya Kramar, L., & Schuldyakov, K. V. (2017). On deterioration mechanism of concrete exposed to freeze–thaw cycles. *IOP Conf Series Materials Science and Engineering, 262*, 012019. https://doi.org/10.1088/1757-899X/262/1/012019
Yang, E. H., Victor, C., & Li, V. C. (2012). Tailoring engineered cementitious composites for impact resistance. *Cement and Concrete Research, 42*(8), 1066–1071. https://doi.org/10.1016/j.cemconres.2012.04.006
Yang, X., & Dai, H. (2020). Effect of geometric form of concrete meso-structure on its mechanical behavior under compression. *Powder Technology, 360*, 372–382. https://doi.org/10.1016/j.powtec.2019.09.049

Yildirim ST, Ekinci CE (2012) Effects on Freeze–Thaw Durability of Fibers in Concrete. https://www.intechopen.com.
Yildirim, S. T., & Ekinci, C. E. (2006). Çelik, cam ve polipropilen lifli betonlarda donma-çözülme etkilerinin araştırılması. *Fırat Üniversitesi Fen Ve Mühendislik Bilimleri Dergisi, 18*(3), 359–366.
Yildirim, S. T., Ekinci, C. E., & Findik, F. (2010). Properties of hybrid fiber reinforced concrete under repeated impact loads. *Russian Journal of Nondestructive Testing, 46*(7), 538–546.
Yildirim, S. T., Meyer, C., & Herfellner, S. (2015). Effects of internal curing on the strength, drying shrinkage and freeze–thaw resistance of concrete containing recycled concrete aggregates. *Construction and Building Materials, 91*, 288–296. https://doi.org/10.1016/j.conbuildmat.2015.05.045.
Zebari, Z., Bedirhanoglu, I., & Aydin, E. (2017). Beton basınç dayanımının ultrasonik ses dalgası yayılma hızı ile tahmin edilmesi. *Dicle Uni. Muhendislik Fakultesi Muhendislik Dergisi, 8*(1), 42–52.
Zhang, P., Sha, D., Li, Q., Zhao, S., & Ling, Y. (2021). Effect of nano silica particles on impact resistance and durability of concrete containing coal fly ash. *Nanomaterials, 11*(5), 1296. https://doi.org/10.3390/nano11051296

Publisher's Note

Cevdet Emin Ekinci is a faculty member at Firat University, Faculty of Technology, Department of Civil Engineering. He received his BS, MS, and PhD degrees from Firat University. He is research interests include concrete, cement, structural damages, bioharmology, and construction technologies.

Belkis Elyigit is a Civil Engineering. She received BS, MS, and PhD degrees from Firat University. She is research interests include concrete, construction technologies, structural damages, bioharmology, and urban transformation.